



Since January 2020 Elsevier has created a COVID-19 resource centre with free information in English and Mandarin on the novel coronavirus COVID-19. The COVID-19 resource centre is hosted on Elsevier Connect, the company's public news and information website.

Elsevier hereby grants permission to make all its COVID-19-related research that is available on the COVID-19 resource centre - including this research content - immediately available in PubMed Central and other publicly funded repositories, such as the WHO COVID database with rights for unrestricted research re-use and analyses in any form or by any means with acknowledgement of the original source. These permissions are granted for free by Elsevier for as long as the COVID-19 resource centre remains active.



SPONTANEOUSLY ARISING DISEASE

Polyarteritis Nodosa in a Cat with Involvement of the Central and Peripheral Nervous Systems

C. Salvadori^{*}, T. Vezzosi[†], V. Marchetti[†] and C. Cantile^{*}

^{*} *Department of Veterinary Sciences, University of Pisa, Viale delle Piagge 2 and* [†] *Ospedale Didattico Veterinario ‘M. Modenato’, Department of Veterinary Sciences, University of Pisa, Via Livornese, San Piero a Grado, Pisa, Italy*

Summary

An 18-month-old neutered male domestic shorthair cat was referred with a history of pyrexia, polyuria and polydipsia, and transient episodes of bilateral hindlimb paralysis. Cardiac evaluation revealed severe systemic hypertension and severe concentric hypertrophy of the left ventricle. One month later the cat had a new episode of hindlimb paralysis with recurrent seizures, and died in status epilepticus. At necropsy examination, the coronary arteries, arcuate renal arteries and common iliac arteries showed marked thickening with nodules segmentally located along the vessels and consequent narrowing of the lumina. Histologically, acute and chronic inflammatory infiltration of the vascular walls was associated with necrosis of the muscular layer. Lesions were consistent with polyarteritis nodosa and involved the small, medium and large arteries of the heart, kidneys, small and large intestine, mesentery, liver and thyroid. Multifocal meningeal vasculitis associated with focal infarction of the frontal lobe and necrotizing vascular polyneuropathy were detected. Involvement of the central and peripheral nervous systems in polyarteritis nodosa is a novel finding in cats.

© 2018 Elsevier Ltd. All rights reserved.

Keywords: cat; peripheral neuropathy; polyarteritis nodosa; vasculitis

Polyarteritis nodosa (PAN) is a systemic necrotizing vasculitis typically involving small- and medium-sized muscular arteries of visceral and soft tissues. PAN can affect every organ, but generally the lungs are spared; venules and capillaries are not involved (Forbess and Bannykh, 2015). In veterinary medicine, PAN is a common disease of laboratory animals, affecting mainly male rats (Lepherd *et al.*, 2013). It has been described in blue foxes (*Alopex lagopus*) (Nordstoga and Westbye, 1976), cynomolgus macaques (*Macaca fascicularis*) (Albassam *et al.*, 1993; Porter *et al.*, 2003), sheep (Landsverk and Bratberg, 1979; Ferreras *et al.*, 2013; Wessel *et al.*, 2017; Pesavento *et al.*, 2018), cattle (Filippich and Mudie, 1972), pigs (Hamir, 1980; Liu *et al.*, 2005), dogs (Carpenter *et al.*, 1988; Snyder *et al.*, 1995) and cats (Altera and Bonasch, 1966; Campbell *et al.*, 1972).

Affected cats were reported to show weight loss, pyrexia, sneezing, leucocytosis, stiffness of all four limbs and muscle pain. Vascular lesions were detected in many organs including the pancreas, thyroid glands, myocardium, lymph nodes, spleen, liver, kidney, lungs, eyes, skeletal muscles and periarticular connective tissue (Altera and Bonasch, 1966; Campbell *et al.*, 1972). Involvement of nervous tissue was not reported.

The pathogenesis of PAN is poorly understood. In man, PAN triggered by virus infections such as with hepatitis B and C viruses, human immunodeficiency virus, parvovirus B19 and hairy cell leukaemia has been described (Ishiguro and Kawashima, 2010; Forbess and Bannykh, 2015). An immune-mediated mechanism in the development of vascular lesions is suspected (Cid *et al.*, 1994; Forbess and Bannykh, 2015) due to the prevalence of macrophages and CD4⁺ T lymphocytes in inflammatory infiltrates and to the clinical response to immunosuppressive

Correspondence to: C. Salvadori (e-mail: claudia.salvadori1@unipi.it).

drugs (Eleftheriou *et al.*, 2013; Watanabe *et al.*, 2016; James *et al.*, 2018). In veterinary medicine, PAN has been described in blue foxes associated with encephalitozoonosis (Nordstoga and Westbye, 1976), in lambs with sarcocystosis (Landsverk and Bratberg, 1979) and in sheep infected with ovine herpesvirus 2 (Pesavento *et al.*, 2018). A relationship with streptococcal infection has been suspected in pigs (Liu *et al.*, 2005). However, no infectious agents have been detected in most cases of PAN in animals (Carpenter *et al.*, 1988; Snyder *et al.*, 1995; Porter *et al.*, 2003; Wessel *et al.*, 2017).

Here we describe the clinical and pathological findings in a case of feline PAN with central and peripheral nervous system involvement not previously reported in the veterinary literature.

An 18-month-old neutered male domestic short-hair cat was referred with a 2-month history of pyrexia, polyuria and polydipsia, vomiting and three episodes of transient bilateral hindlimb paralysis. During the last year, recurrent vomiting and diarrhoea were reported. The cat was vaccinated and there was no history of exposure to toxins. The cat was seronegative for feline infectious peritonitis (FIP), feline leukaemia virus (FeLV), feline immunodeficiency virus (FIV) and *Toxoplasma gondii*. On presentation, the cat was bright, alert and responsive, with a low body condition score (3/9). Cardiac auscultation revealed a systolic heart murmur (grade 3/6) with maximal intensity over the sternum and severe systemic hypertension (systolic blood pressure 230 mm Hg; normal range 120–150 mm Hg). Echocardiography revealed severe concentric hypertrophy of the left ventricle with heterogeneous echogenicity of the myocardium, a left atrium of normal dimensions and a dynamic obstruction of the right ventricular outflow tract. Abdominal ultrasonography revealed chronic intestinal and pancreatic inflammation. Neurological examination was unremarkable. Complete blood count and coagulation profile were normal. Serum electrophoresis showed a moderate hyperproteinaemia (9 g/dl, reference interval 6–8 g/dl) with alpha-2 hyperglobulinaemia. Serum cardiac troponin I was 0 ng/ml (reference interval 0–0.11 ng/ml) and concentrations of cobalamin and folate were normal. Low urine specificity gravity (1.012; reference interval 1.035–1.060) was also detected. After these diagnostic investigations, the cat was discharged on amlodipine 0.2 mg/kg q24h for systemic hypertension, clopidogrel 1 mg/kg q24h as an antithrombotic drug, probiotics (feline Fortiflora[®] ProPlan[®] Veterinary Diets; Nestlé Purina, St. Louis, Missouri, USA) and a gastrointestinal diet (feline EN Gastrointestinal[™] Pro Plan[®] Veterinary Diets; Nestlé Purina). After 1 week of therapy, the cat appeared to

have improved clinically, but the systolic blood pressure was still high, and the dose of amlodipine was increased to 0.2 mg/kg q12h. One month later the cat was readmitted with a new episode of hindlimb paralysis with bilateral loss of patellar reflex and reduced nociception. The cat also showed circling, vocalization and recurrent seizures. The cat died in status epilepticus on the same day.

A complete necropsy examination was performed and gross changes were evident in the heart, kidneys and at the aortic bifurcation into the common iliac arteries. Coronary arteries, mainly the left coronary artery and its branches, showed marked thickening with small nodules located segmentally along the vessel (Fig. 1). In transverse sections, moderate symmetrical thickening of the left ventricular free wall and interventricular septum with narrowing of the lumen were evident; coronary arteries showed severe thickening and hardening of the walls with marked narrowing of the lumina. No haemorrhages were detected, but there was multifocal pale discolouration of the myocardium. The kidneys showed an irregular surface with multifocal pale scars. Thinning and discolouration of the cortex and marked thickening of the arcuate arteries, with these vessels having a tortuous course and segmental nodular change, were evident on longitudinal sections of both kidneys



Fig. 1. Heart. The left coronary artery and its branches show severe thickening and small nodules located segmentally. Bar, 1 cm.

(Supplementary Fig. 1). Segmental nodular thickening was also evident in the common iliac arteries (especially that of the right side) and at the terminal bifurcation of the aorta. Samples of major organs, the aortic and iliac arteries and the entire central nervous system (CNS) were fixed in 4% phosphate buffered formalin. Samples of the right and left cranial tibial and triceps muscles were snap frozen in isopentane precooled in liquid nitrogen and samples of the right and left peroneal common nerves and ulnar nerves were fixed in 2.5% glutaraldehyde in 0.1 M phosphate buffer at 4°C.

Formalin-fixed tissues were processed routinely and embedded in paraffin wax. Sections were stained with haematoxylin and eosin (HE), periodic acid–Schiff (PAS), Luxol fast blue, Gomori's trichrome, orcein and Perls' Prussian blue methods. Selected sections were labelled immunohistochemically with antibodies specific for CD3 (clone F7.2.38; 1 in 100 dilution; Dako, Glostrup, Denmark), CD20 (RB9013; 1 in 400 dilution; Thermo Scientific, Fremont, California, USA), Iba-1 (1 in 300 dilution; Wako, Osaka, Japan), major histocompatibility complex class II (MHC class II; clone 1AL.1B5; 1 in 10 dilution; Dako), feline IgG, IgM and complement factor C3 (each 1 in 10 dilution; Binding Site, Birmingham, UK), feline coronavirus (FIPV3-70; 1 in 200 dilution; OriGene Technologies Inc., Rockville, Maryland, USA) and smooth muscle actin (clone 1A4; 1 in 500 dilution; Dako). Cryostat sections (8 µm) of frozen muscle were evaluated using a standard panel of histochemical stains and enzyme reactions (Salvadori *et al.*, 2012). Nerves were post-fixed in osmium tetroxide, dehydrated in ethanol and embedded in epoxy resin. Semithin sections were stained with toluidine blue and methylene blue/basic fuchsin methods.

Microscopical examination revealed multifocal peri- and panarteritis involving small, medium and large arteries of the heart, kidney, small and large intestine, mesentery, liver, thyroid gland, brain and spinal meninges (Fig. 2), and peripheral nerves (Fig. 3). Inflammatory cells, mainly MHC class II-positive cells, with higher numbers of T lymphocytes (Supplementary Fig. 2) and macrophages (Supplementary Fig. 3) and fewer CD20-positive lymphocytes, plasma cells and rare neutrophils, infiltrated the adventitia and perivascular tissues, spreading within the artery wall to the subendothelial layer. Both IgG- and IgM-labelled plasma cells were evident, but no C3 was detected. Inflammatory cell infiltration was associated with necrosis and loss of smooth muscle fibres of the tunica media and delamination and disintegration of the internal and external elastic laminae (Supplementary Figs. 4 and 5).

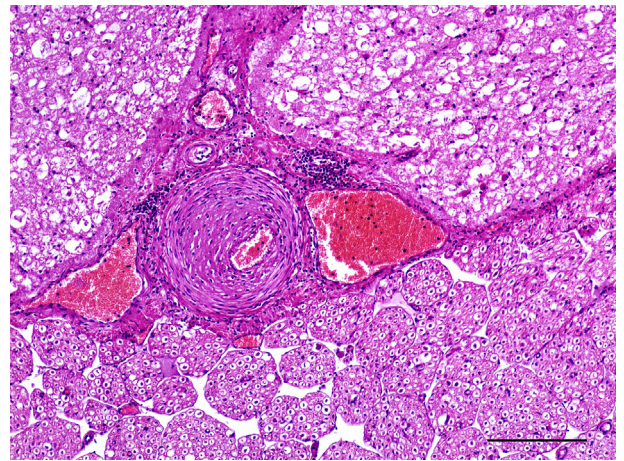


Fig. 2. Lumbar spinal cord. The ventral spinal artery shows severe thickening of the intima and tunica media with narrowing of the lumen. Perivascular inflammatory infiltrates are mainly composed of lymphocytes. White matter degeneration of ventral funiculi is also evident. HE. Bar, 200 µm.

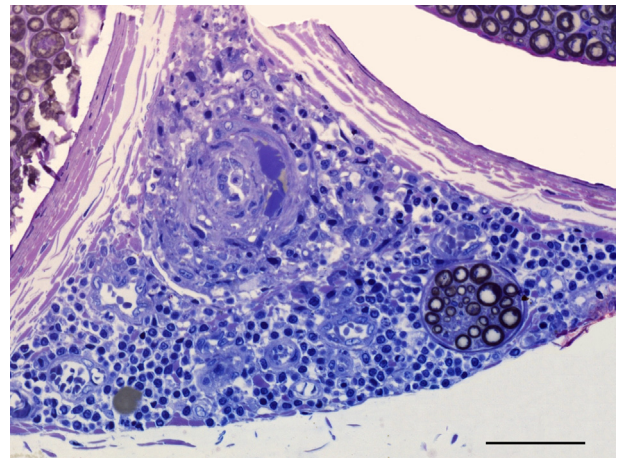


Fig. 3. Peroneal nerve. Moderate thickening with fibrinoid necrosis of a small epineurial arteriole. Adventitial, perivascular and epineurial inflammatory infiltrates are mainly composed of lymphocytes and macrophages and are accompanied by epineurial oedema. Epoxy embedded tissue, semithin section. Methylene blue–basic fuchsin stain. Bar, 50 µm.

Different stages of vascular inflammation were evident in the same tissue and the coexistence of affected and unaffected vessels was common. Acute stages, with fibrinoid necrosis of the tunica media and a dominant infiltration of neutrophils (Supplementary Fig. 6), were associated with chronic stages characterized by severe thickening of the arterial wall and narrowing of the lumen. In severely thickened vessels, both the intima and tunica media showed marked proliferation of fibroblasts and hyperplasia and hypertrophy of smooth muscle (Fig. 4),

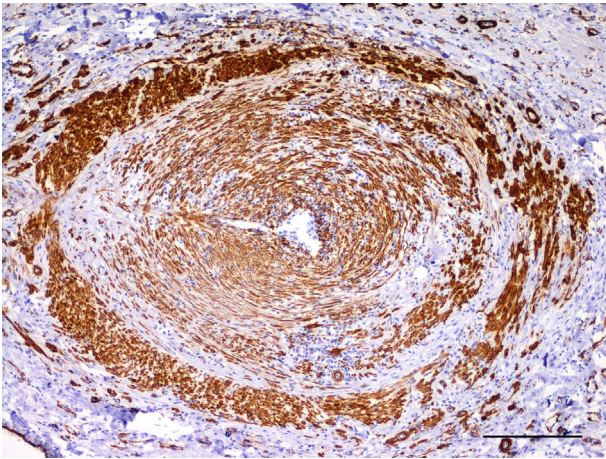


Fig. 4. Heart. Hyperplasia and hypertrophy of smooth muscle fibres is evident within the intima and tunica media of a medium calibre artery. Inflammatory cells infiltrate and dissect the muscular layer. IHC, anti-SMA antibody. Bar, 200 μ m.

with extracellular oedema. Intramural neovascularization was also evident. Rarely, intraluminal thrombi and haemosiderin-laden macrophages, suggesting previous haemorrhage, were evident.

The most severe vascular lesions were detected in the heart. Coronary arteries and all of their branches in the myocardium showed severe inflammatory changes associated with marked thickening of arterial walls. Multifocal to coalescing fibrosis was also evident in the perimysial and endomysial connective tissue of the myocardium.

In both kidneys, severe vascular lesions were associated with multifocal interstitial nephritis and fibrosis without involvement of the glomeruli. In the small and large intestine, arterial vessels of the external and internal muscular layers were mainly affected. In the CNS, both the dura mater and leptomeninges were involved, with scattered vascular lesions, mainly located in the spinal cord and ventral aspect of the thalamus, midbrain, medulla oblongata and frontal lobes. Lesions were accompanied by scattered inflammatory cells in the meninges and a focal infarct in the ventral frontal cortex. This latter lesion was associated with affected vessels of the meninges and was characterized by malacia and white matter degeneration, gliosis and infiltration of macrophages laden with haemosiderin. Both ulnar and common peroneal nerves showed different stages of inflammation of epineural small and medium arteries, ranging from mild perivascular mononuclear cell infiltration to severe thickening of the intima and tunica media with destruction of the elastic lamina (Fig. 3 and Supplementary Fig. 5). Vascular lesions were associated with axonal degeneration and a slight loss of

large and medium myelinated fibres of nerve fascicles. In muscle samples, there was moderate variation in muscle fibre size and shape, mainly in the cranial tibial muscle, in which there were many angular or rounded atrophic fibres and rare hypertrophic fibres. Rounded atrophic fibres were frequently observed at the periphery of muscle fascicles. No fibrosis or inflammatory infiltrates were observed in the muscle samples. Myofibre type distribution and enzymatic oxidative pattern were normal. No lesions were observed in the lungs and no intralesional bacteria, protozoa or fungi were identified in any tissues. Immunolabelling for FIP coronavirus antigen was negative in all tissues.

The pathological findings in this cat were consistent with PAN as described previously in cats and in other species (Altera and Bonasch, 1966; Campbell *et al.*, 1972; Albassam *et al.*, 1993; Porter *et al.*, 2003; Ferreras *et al.*, 2013). Involvement of the lungs and eyes was absent, in contrast with other reported feline cases (Altera and Bonasch, 1966; Campbell *et al.*, 1972). Although some authors proposed the term 'systemic necrotizing arteritis' instead of PAN (Robinson and Robinson, 2016), the present cat showed lesions strongly resembling those described in human patients. Involvement of small- and medium-sized arteries showing severe segmental nodular thickening with marked perivascular and intramural mononuclear inflammatory cell infiltration, as well as the presence of affected and unaffected blood vessels within the same tissue, sparing of the lungs, and preference for arterial branching, are all specific features of human PAN (Forbess and Bannykh, 2015).

A prevalence of T lymphocytes and macrophages with a high number of MHC II-labelled cells and scattered IgM- and IgG-labelled plasma cells was detected in our cat as previously described (Porter *et al.*, 2003; Liu *et al.*, 2005; Ferreras *et al.*, 2013). A cell-mediated immune mechanism was suspected, similar to that described in man (Cid *et al.*, 1994). Although no complement deposition was detected, an immune complex-mediated disorder could not be excluded. Indeed, the observed lesions could result from a progression of immune mechanisms from type III to type IV hypersensitivity. Prolonged inflammatory vascular injury stimulates proliferation of smooth muscle cells, deposits of extracellular matrix and fibroblast growth with progressive intimal and medial thickening and narrowing of the vascular lumen (Schoen, 2005). In cats, severe systemic vasculitis involving the CNS is frequently caused by FIP coronavirus, but these lesions differ from those observed in the present cat and there was no evidence of coronavirus antigen in the tissues examined. Pyogranulomatous vasculitis in FIP mainly involves small-

and medium-sized veins and inflammatory cells are mainly monocytes/macrophages with a few neutrophils and lymphocytes (Kipar *et al.*, 2005).

The clinical signs of neurological, cardiac and renal dysfunction shown by the present cat were a consequence of vascular damage and related vascular hypoxia. Left ventricular concentric hypertrophy with heterogeneous echogenicity of the myocardium was assumed to be a consequence of chronic systemic hypertension, severe vascular inflammatory lesions and myocardial fibrosis (Abbott, 2010). Although PAN involving the coronary arteries, with subsequent myocardial infarction, has been described in man and dogs (Carpenter *et al.*, 1988; Odhav *et al.*, 1994; Yuce *et al.*, 2011), no clinical signs of acute coronary syndrome were identified, and no haemorrhages or infarcts were detected on post-mortem examination in the present case. Central neurological signs, such as circling and seizures, were likely due to involvement of the meningeal vessels and the presence of cerebral infarction as described in sows and dogs with PAN (Carpenter *et al.*, 1988; Liu *et al.*, 2005). The present cat also showed hindlimb paralysis subsequent to necrotizing vascular neuropathy. Nerve fibre degeneration was secondary to ischaemia due to vasculitis of the vasa nervorum. In cats, hindlimb paralysis with decreased peripheral pulse pressure, pallor and coolness frequently results from aortic thromboembolism secondary to underlying cardiac disease, most commonly hypertrophic cardiomyopathy, but has also been observed in peripheral arterial neoplasia or foreign body embolization (Dickinson and LeCouteur, 2004). Necrotizing vascular neuropathies secondary to PAN are common in man (Imboden, 2017; James *et al.*, 2018), but have not been described in veterinary medicine. Peripheral nerve involvement was associated with neurogenic muscle atrophy and primary myopathic findings, such as perifascicular atrophy, were suggestive of ischaemic myopathy.

In conclusion, PAN should be included in the differential diagnoses of cardiovascular and neurological syndromes in cats. Combined muscle and nerve biopsy could provide useful clues for ante-mortem diagnosis of feline PAN.

Acknowledgments

We thank Mrs L. Baroncini for expert technical assistance in histopathology.

Conflict of Interest Statement

The authors declare no conflict of interest with respect to the publication of this manuscript.

Supplementary data

Supplementary data to this article can be found online at <https://doi.org/10.1016/j.jcpa.2018.11.003>.

References

- Abbott JA (2010) Feline hypertrophic cardiomyopathy: an update. *Veterinary Clinics of North America: Small Animal Practice*, **40**, 685–700.
- Albassam MA, Lillie LE, Smith GS (1993) Asymptomatic polyarteritis in a cynomolgus monkey. *Laboratory Animal Science*, **43**, 628–629.
- Altera KP, Bonasch H (1966) Periarteritis nodosa in a cat. *Journal of the American Veterinary Medical Association*, **149**, 1307–1311.
- Campbell LH, Fox JG, Drake DF (1972) Ocular and other manifestation of periarteritis nodosa in a cat. *Journal of the American Veterinary Medical Association*, **161**, 1122–1126.
- Carpenter JL, Moore FM, Albert DM (1988) Polyarteritis nodosa and rheumatic heart disease in a dog. *Journal of the American Veterinary Medical Association*, **192**, 929–932.
- Cid MC, Grau JM, Casademont J, Campo E, Coll-Vinent B *et al.* (1994) Immunohistochemical characterization of inflammatory cells and immunologic activation markers in muscle and nerve biopsy specimens from patients with systemic polyarteritis nodosa. *Arthritis & Rheumatism*, **37**, 1055–1061.
- Dickinson PJ, LeCouteur RA (2004) Feline neuromuscular disorders. *Veterinary Clinics of North America: Small Animal Practice*, **34**, 1307–1359.
- Eleftheriou D, Dillon MJ, Tullus K, Marks SD, Pilkington CA *et al.* (2013) Systemic polyarteritis nodosa in the young: a single-center experience over thirty-two years. *Arthritis & Rheumatism*, **65**, 2476–2486.
- Ferreras MC, Benavides J, Fuertes M, García-Pariente C, Muñoz M *et al.* (2013) Pathological features of systemic necrotizing vasculitis (polyarteritis nodosa) in sheep. *Journal of Comparative Pathology*, **149**, 74–81.
- Filippich LJ, Mudie AW (1972) Polyarteritis nodosa in a bovine carcass. *Australian Veterinary Journal*, **48**, 66.
- Forbess L, Bannykh S (2015) Polyarteritis nodosa. *Rheumatic Disease Clinics of North America*, **41**, 33–46.
- Hamir AN (1980) Polyarteritis nodosa in a sow. *Australian Veterinary Journal*, **56**, 343–344.
- Imboden JB (2017) Involvement of the peripheral nervous system in polyarteritis nodosa and antineutrophil cytoplasmic antibody-associated vasculitis. *Rheumatic Disease Clinics of North America*, **43**, 633–639.
- Ishiguro N, Kawashima M (2010) Cutaneous polyarteritis nodosa: a report of 16 cases with clinical and histopathological analysis and a review of the published work. *Journal of Dermatology*, **37**, 85–93.
- James J, Jose J, Thulaseedharan NK (2018) Acute necrotizing vasculitic neuropathy due to polyarteritis nodosa. *Oman Medical Journal*, **33**, 253–255.
- Kipar A, May H, Menger S, Weber M, Leukert W *et al.* (2005) Morphologic features and development of

- granulomatous vasculitis in feline infectious peritonitis. *Veterinary Pathology*, **42**, 321–330.
- Landsverk T, Bratberg B (1979) Polyarteritis nodosa associated with sarcocystosis in a lamb. *Acta Veterinaria Scandinavica*, **20**, 306–308.
- Lepherd ML, Schlafer DH, De Matos R, Southard TL (2013) Pathology in practice. Polyarteritis nodosa. *Journal of the American Veterinary Medical Association*, **243**, 1399–1401.
- Liu CH, Chiang YH, Chu RM, Pang VF, Lee CC (2005) High incidence of polyarteritis nodosa in the brains of culled sows. *Journal of Veterinary Medical Science*, **67**, 125–127.
- Nordstoga K, Westbye K (1976) Polyarteritis nodosa associated with nosematosis in blue foxes. *Acta Pathologica Microbiologica Scandinavica*, **84**, 291–296.
- Odhav S, McKown K, Lohr KM (1994) Polyarteritis nodosa presenting as recurrent myocardial infarction. *Chest*, **105**, 1615.
- Pesavento PA, Dange RB, Ferreras MC, Dasjerdi A, Pérez V *et al.* (2018) Systemic necrotizing vasculitis in sheep is associated with ovine herpesvirus 2. *Veterinary Pathology*, <https://doi.org/10.1177/0300985818795166> (Epub ahead of print).
- Porter BF, Frost P, Hubbard GB (2003) Polyarteritis nodosa in a cynomolgus macaque (*Macaca fascicularis*). *Veterinary Pathology*, **40**, 570–573.
- Robinson WF, Robinson NA (2016) Cardiovascular system. In: *Jubb, Kennedy, and Palmer's Pathology of Domestic Animals*, 6th Edit., MG Maxie, Ed., Elsevier Saunders, St. Louis, p. 71.
- Salvadori C, Vattemi G, Marini M, Bocchese E, Tomelleri G *et al.* (2012) Adult-onset muscular dystrophy in a cat associated with a presumptive alteration in trafficking of caveolin-3. *Journal of Comparative Pathology*, **147**, 253–258.
- Schoen FJ (2005) Blood vessels. In: *Robbins' and Cotran's Pathologic Basis of Disease*, 7th Edit., V Kumar, AK Abbas, N Fausto, Eds., Elsevier Saunders, Philadelphia, pp. 511–554.
- Snyder PW, Kazacos EA, Scott-Moncrieff JC, HogenEsch H, Carlton WW *et al.* (1995) Pathologic features of naturally occurring juvenile polyarteritis in beagle dogs. *Veterinary Pathology*, **32**, 337–345.
- Watanabe K, Rajderkar DA, Modica RF (2016) A case of polyarteritis nodosa associated with vertebral artery vasculitis treated successfully with tocilizumab and cyclophosphamide. *Case Reports in Pediatrics* 7987081.
- Wessel M, Strugnell B, Woodger N, Peat M, La Rocca SA *et al.* (2017) Systemic necrotizing polyarteritis in three weaned lambs from one flock. *Journal of Veterinary Diagnostic Investigation*, **29**, 733–737.
- Yuce M, Davutoglu V, Sari I, Onat AM (2011) Polyarteritis nodosa with multiple coronary aneurysms presenting as acute myocardial infarction. *The American Journal of the Medical Sciences*, **341**, 409.

[Received, October 11th, 2018
Accepted, November 15th, 2018]